

A procedure for the calculation of the natural gas molar heat capacity, the isentropic exponent, and the Joule–Thomson coefficient

Ivan Marić*

Ruder Bošković Institute, Division of Electronics, Laboratory for Information Systems, Bijenička c. 54, P.O.B. 180, 10002 Zagreb, Croatia

Received 22 March 2006; received in revised form 19 September 2006; accepted 14 December 2006

Abstract

A numerical procedure for the computation of a natural gas molar heat capacity, the isentropic exponent, and the Joule–Thomson coefficient has been derived using fundamental thermodynamic equations, DIPPR AIChE generic ideal heat capacity equations, and AGA-8 extended virial-type equations of state. The procedure is implemented using the Object-Oriented Programming (OOP) approach. The results calculated are compared with the corresponding measurement data. The flow-rate through the orifice plate with corner taps is simulated and the corresponding error due to adiabatic expansion is calculated. The results are graphically illustrated and discussed.

© 2007 Elsevier Ltd. All rights reserved.

Keywords: Heat capacity; Joule–Thomson coefficient; Isentropic exponent; Natural gas; Flow measurement

1. Introduction

When a gas is forced to flow through a differential device (see Fig. 1) it expands to a lower pressure and changes its density. Flow-rate equations for differential pressure meters assume a constant density of a fluid within the meter. This assumption applies only to incompressible flows. In the case of compressible flows, a correction must be made. This correction is known as the adiabatic expansion factor, which depends on several parameters including the differential pressure, the absolute pressure, pipe diameter, the differential device bore diameter, and the isentropic exponent. The isentropic exponent has a limited effect on the adiabatic correction factor, but needs to be calculated if accurate flow-rate measurements are needed.

When a gas expands through a restriction to a lower pressure, it also changes its temperature. This process occurs under the conditions of constant enthalpy and is known as Joule–Thomson expansion [1]. It can also be considered as an adiabatic effect, because the pressure change occurs too quickly for significant heat transfer to take place. The temperature change is related to pressure change and is characterized by the Joule–Thomson coefficient. The temperature drop increases

with the increase of the pressure drop and is proportional to the Joule–Thomson coefficient. According to [2], the upstream temperature is used for the calculation of flow-rates, but the temperature is preferably measured downstream of the differential device. The use of downstream instead of upstream temperatures may cause a flow-rate measurement error due to the difference in the gas density caused by the temperature change. Our objective is to derive the numerical procedure for the calculation of the natural gas specific heat capacity, the isentropic exponent, and the Joule–Thomson coefficient that can be used to compensate for the adiabatic expansion effects in real-time flow-rate measurements.

2. Procedure

This section outlines the procedure for the calculation of specific heat capacities at a constant pressure c_p and at a constant volume c_v , the Joule–Thomson coefficient μ_{JT} , and the isentropic exponent κ of a natural gas based on thermodynamic equations, AGA-8 extended virial type characterization equations [3,4], and DIPPR generic ideal heat capacity equations [5]. First, the relation of the molar heat capacity at constant volume to the equation of state will be derived. Then the relation will be used to calculate a molar heat capacity at constant pressure, which will then be used

* Tel.: +385 1 4561191; fax: +385 1 4680114.

E-mail address: ivan.maric@irb.hr.

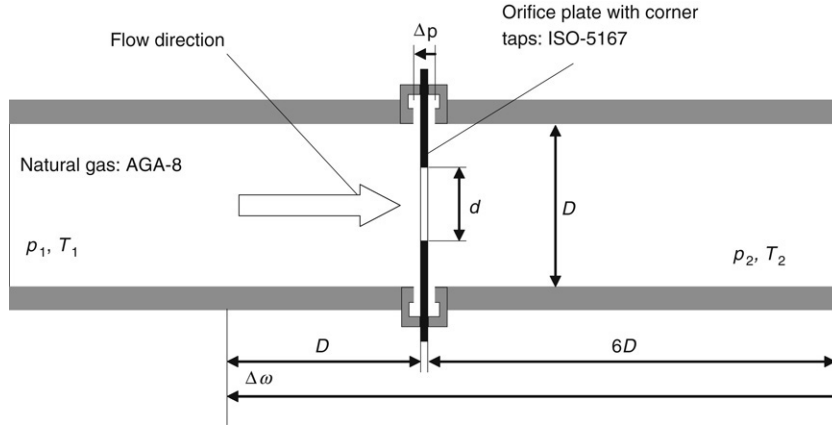


Fig. 1. Schematic diagram of the gas flow-rate measurement using an orifice plate with corner taps.

for the calculation of the Joule–Thomson coefficient and the isentropic exponent. The total differential for entropy, related to temperature and molar volume [6], is:

$$ds = \left(\frac{\partial s}{\partial T} \right)_{v_m} dT + \left(\frac{\partial s}{\partial v_m} \right)_T dv_m, \quad (1)$$

where s denotes entropy, T denotes temperature, and v_m is a molar volume of a gas. By dividing the fundamental differential for internal energy $du = T \cdot ds - p \cdot dv_m$ by dT while holding v_m constant, the coefficient of dT in Eq. (1) becomes $c_{m,v}/T$ since the molar heat at constant volume is defined by $c_{m,v} = (\partial u/\partial T)_{v_m}$. The Maxwell relation $(\partial s/\partial v_m)_T = (\partial p/\partial T)_{v_m}$, is used to substitute the coefficient of dv_m . Finally, the Eq. (1) becomes:

$$ds = \frac{c_{m,v}}{T} dT + \left(\frac{\partial p}{\partial T} \right)_{v_m} dv_m. \quad (2)$$

Similarly, starting from a total differential for entropy related to temperature and pressure [6] $ds = (\partial s/\partial T)_p dT + (\partial s/\partial p)_T dp$ and by dividing the fundamental differential for enthalpy $dh = T \cdot ds + v_m \cdot dp$ by dT while holding p constant, the coefficient of dT in the total differential becomes $c_{m,p}/T$, since the molar heat capacity at constant pressure is defined by $c_{m,p} = (\partial h/\partial T)_p$. The Maxwell relation $(\partial s/\partial p)_T = (\partial v_m/\partial T)_p$ is used to substitute the coefficient of dp and the following relation is obtained:

$$ds = \frac{c_{m,p}}{T} dT + \left(\frac{\partial v_m}{\partial T} \right)_p dp. \quad (3)$$

Subtracting Eq. (2) from Eq. (3), and then dividing the resulting equation by dv_m while holding p constant, and finally inverting the partial derivative $(\partial T/\partial v_m)_p$, the following equation is obtained:

$$c_{m,p} - c_{m,v} = T \left(\frac{\partial v_m}{\partial T} \right)_p \left(\frac{\partial p}{\partial T} \right)_{v_m}. \quad (4)$$

The total differential of the thermodynamic property Eqs. (2) and (3) must be the exact differential, i.e. the order of forming the mixed second derivative is irrelevant. The partial derivative of the first coefficient with respect to the second

variable equals to the partial derivative of the second coefficient with respect to the first variable. By applying this property to Eq. (2) and by assuming T to be the first variable with the corresponding coefficient $c_{m,v}/T$, and v_m the second variable with the corresponding coefficient $(\partial p/\partial T)_{v_m}$, we obtain:

$$\left(\frac{\partial c_{m,v}}{\partial v_m} \right)_T = T \left(\frac{\partial^2 p}{\partial T^2} \right)_{v_m}. \quad (5)$$

The Eq. (5) can be rewritten in the following integral form:

$$c_{m,v} = c_{m,vI} + T \int_{v_{mI} \rightarrow \infty (T=\text{const})}^{v_m} \left(\frac{\partial^2 p}{\partial T^2} \right)_{v_m} dv_m \quad (6)$$

where $c_{m,vI}$, v_{mI} , and v_m denote the ideal molar heat capacity at constant volume, the corresponding molar volume of the ideal, and the real gas at temperature T respectively. Real gases behave more like ideal gases as the pressure approaches zero or $v_{mI} \rightarrow \infty$. After substituting $v_m = 1/\rho_m$, $p = RTZ\rho_m$ and $c_{m,vI} = c_{m,pI} - R$, the Eq. (6) transforms to:

$$c_{m,v} = c_{m,pI} - R - RT \times \int_{\rho_{mI} \rightarrow 0 (T=\text{const})}^{\rho_m} \frac{1}{\rho_m} \left(2 \left(\frac{\partial Z}{\partial T} \right)_{\rho_m} + T \left(\frac{\partial^2 Z}{\partial T^2} \right)_{\rho_m} \right) d\rho_m \quad (7)$$

where $c_{m,pI}$ denotes the temperature dependent molar heat capacity of the ideal gas at constant pressure, R is the universal gas constant, Z is the compression factor, and ρ_{mI} and ρ_m are the corresponding molar densities of the ideal and the real gas at temperature T . After substituting the first and the second derivative of the AGA-8 compressibility equation [4],

$$Z = 1 + B\rho_m - \rho_r \sum_{n=13}^{18} C_n^* + \sum_{n=13}^{58} C_n^* \left(b_n - c_n k_n \rho_r^{k_n} \right) \rho_r^{b_n} e^{-c_n \rho_r^{k_n}} \quad (8)$$

into the Eq. (7) and after integration we obtain

$$c_{m,v} = c_{m,pI} - R + RT\rho_r (2C_0 + TC_1 - C_2) \quad (9)$$

with

$$C_0 = \sum_{n=13}^{18} C_n^{*'} - \frac{B'}{K^3} \quad (10)$$

$$C_1 = \sum_{n=13}^{18} C_n^{*''} - \frac{B''}{K^3} \quad (11)$$

$$C_2 = \sum_{n=13}^{58} (2C_n^{*'} + TC_n^{*''}) \rho_r^{b_n-1} e^{-c_n \rho_r^{k_n}} \quad (12)$$

where ρ_r is the reduced density ($\rho_r = K^3 \rho_m$), B is the second virial coefficient, $\{C_n^*\}$ are the temperature dependent coefficients, K is the mixture size parameter, while $\{b_n\}$, $\{c_n\}$, and $\{k_n\}$ are the parameters of the equation of state. The mixture size parameter K is calculated using the following equation [4]:

$$K^5 = \left(\sum_{i=1}^N y_i K_i^{5/2} \right)^2 + 2 \sum_{i=1}^{N-1} \sum_{j=i+1}^N y_i y_j (K_{ij}^5 - 1) (K_i K_j)^{5/2}, \quad (13)$$

where y_i denotes the molar fraction of the component i , while $\{K_i\}$ and $\{K_{ij}\}$ are the corresponding size parameters and the binary interaction parameters given in [4]. According to [4], the second virial coefficient is calculated using the following equation:

$$B = \sum_{n=1}^{18} a_n T^{-u_n} \sum_{i=1}^N \sum_{j=1}^N y_i y_j B_{nij}^* E_{ij}^{u_n} (K_i K_j)^{3/2} \quad (14)$$

and the coefficients $\{B_{nij}^*\}$, $\{E_{ij}\}$ and $\{G_{ij}\}$ are defined by

$$B_{nij}^* = (G_{ij} + 1 - g_n)^{g_n} (Q_i Q_j + 1 - q_n)^{q_n} \times (F_i^{1/2} F_j^{1/2} + 1 - f_n)^{f_n} \cdot (S_i S_j + 1 - s_n)^{s_n} (W_i W_j + 1 - w_n)^{w_n}, \quad (15)$$

$$E_{ij} = E_{ij}^* (E_i E_j)^{1/2} \quad (16)$$

and

$$G_{ij} = G_{ij}^* (G_i + G_j)/2, \quad (17)$$

where T is the temperature, N is the total number of gas mixture components, y_i is the molar fraction of the component i , $\{a_n\}$, $\{f_n\}$, $\{g_n\}$, $\{q_n\}$, $\{s_n\}$, $\{u_n\}$, and $\{w_n\}$ are the parameters of the equation of state, $\{E_i\}$, $\{F_i\}$, $\{G_i\}$, $\{K_i\}$, $\{Q_i\}$, $\{S_i\}$, and $\{W_i\}$ are the corresponding characterization parameters, while $\{E_{ij}^*\}$ and $\{G_{ij}^*\}$ are the corresponding binary interaction parameters. The main symbols and units are given in Table 1. For additional symbols and units refer to ISO-12213-2 [4]. The temperature dependent coefficients $\{C_n^*; n = 1, \dots, 58\}$ and the mixture parameters U , G , Q , and F are calculated using the equations [4]:

$$C_n^* = a_n (G + 1 - g_n)^{g_n} (Q^2 + 1 - q_n)^{q_n} \times (F + 1 - f_n)^{f_n} U^{u_n} T^{-u_n}, \quad (18)$$

Table 1

Symbols and units (for additional symbols and units refer to ISO-12213-2 [4])

| Symbol | Description | Unit |
|-----------------|--|---------------------------------|
| B | Second virial coefficient | $\text{m}^3 * \text{kmol}^{-1}$ |
| B_{nij}^* | Mixture interaction coefficient | – |
| C | Coefficient of discharge | – |
| $c_{m,p}$ | Molar heat capacity at constant pressure | $\text{J}/(\text{mol K})$ |
| $c_{m,v}$ | Molar heat capacity at constant volume | $\text{J}/(\text{mol K})$ |
| C_n^* | Temperature and composition dependent coefficients | – |
| c_n | AGA-8 equation of state parameter | – |
| c_p | Specific heat capacity at constant pressure | $\text{J}/(\text{kg K})$ |
| $c_{m,pI}$ | Ideal molar heat capacity of the natural gas mixture | $\text{J}/(\text{mol K})$ |
| $C_{m,pI}^j$ | Ideal molar heat capacity of the gas component j | $\text{J}/(\text{mol K})$ |
| D | Upstream internal pipe diameter | m |
| d | Diameter of orifice | m |
| h | Specific enthalpy | J/kg |
| K | Size parameter | – |
| p | Absolute pressure | Pa |
| q_m | Mass flow-rate | kg/s |
| R | Molar gas constant 8314.51 | $\text{J}/(\text{kmol K})$ |
| s | Specific entropy | $\text{J}/(\text{kg K})$ |
| T | Absolute temperature | K |
| v_m | Molar specific volume | m^3/kmol |
| v_{mI} | Molar specific volume of ideal gas | m^3/kmol |
| y_i | Molar fraction of i -th component in gas mixture | – |
| Z | Compression factor | – |
| β | Diameter ratio d/D | – |
| Δp | Differential pressure | Pa |
| $\Delta \omega$ | Pressure loss | Pa |
| κ | Isentropic exponent | – |
| μ_{JT} | Joule–Thomson coefficient | K/Pa |
| ρ_m | Molar density | kmol/m^3 |
| ρ_{mI} | Molar density of ideal gas | kmol/m^3 |
| ρ_r | Reduced density | – |

$$U^5 = \left(\sum_{i=1}^N y_i E_i^{5/2} \right)^2 + 2 \sum_{i=1}^{N-1} \sum_{j=i+1}^N y_i y_j (U_{ij}^5 - 1) (E_i E_j)^{5/2}, \quad (19)$$

$$G = \sum_{i=1}^N y_i G_i + 2 \sum_{i=1}^{N-1} \sum_{j=i+1}^N y_i y_j (G_{ij}^* - 1) (G_i + G_j), \quad (20)$$

$$Q = \sum_{i=1}^N y_i Q_i, \quad (21)$$

and

$$F = \sum_{i=1}^N y_i^2 F_i, \quad (22)$$

where, U_{ij} is the binary interaction parameter for mixture energy. The first and the second derivatives of the coefficients B and C_n^* , with respect to temperature, are:

$$B' = - \sum_{n=1}^{18} a_n u_n T^{-u_n-1} \sum_{i=1}^N \sum_{j=1}^N y_i y_j B_{nij}^* E_{ij}^{u_n} (K_i K_j)^{3/2} \quad (23)$$

Table 2
The DIPPR/AIChE gas heat capacity constants

| Natural gas component | DIPPR/AIChE ideal gas heat capacity constants | | | | |
|---|---|----------|----------|----------|----------|
| | <i>a</i> | <i>b</i> | <i>c</i> | <i>d</i> | <i>e</i> |
| Methane — CH ₄ | 33 298 | 79 933 | 2086.9 | 41 602 | 991.96 |
| Ethane — C ₂ H ₆ | 40 326 | 134 220 | 1655.5 | 73 223 | 752.87 |
| Propane — C ₃ H ₈ | 51 920 | 192 450 | 1626.5 | 116 800 | 723.6 |

$$B'' = \sum_{n=1}^{18} a_n u_n (u_n + 1) T^{-u_n - 2} \times \sum_{i=1}^N \sum_{j=1}^N y_i y_j B_{nij}^* E_{ij}^{u_n} (K_i K_j)^{3/2} \quad (24)$$

$$C_n^{*'} = -\frac{u_n}{T} C_n^* \quad (25)$$

$$C_n^{*''} = -\frac{u_n + 1}{T} C_n^{*'} \quad (26)$$

The ideal molar heat capacity c_{pI} is calculated by

$$c_{m,pI} = \sum_{j=1}^N y_j c_{m,pi}^j \quad (27)$$

where y_j is the molar fraction of component j in the gas mixture and $C_{m,pi}^j$ is the molar heat capacity of the same component. The molar heat capacities of the ideal gas mixture components can be approximated by the DIPPR/AIChE generic equations [5], i.e.

$$c_{m,pi}^j = a_j + b_j \left(\frac{c_j/T}{\sinh(c_j/T)} \right)^2 + d_j \left(\frac{e_j/T}{\cosh(e_j/T)} \right)^2, \quad (28)$$

where $c_{m,pi}^j$ is the molar heat capacity of the component j of the ideal gas mixture, a_j , b_j , c_j , d_j , and e_j are the corresponding constants, and T is the temperature. The constants a , b , c , d , and e for some gases are shown in Table 2.

The partial derivative of pressure with respect to temperature at constant molar volume, and the partial derivative of molar volume with respect to temperature at constant pressure, are defined by the equations:

$$\left(\frac{\partial p}{\partial T} \right)_{v_m} = R \rho_m [Z + T(C_3 - \rho_r C_0)] \quad (29)$$

and

$$\left(\frac{\partial v_m}{\partial T} \right)_p = \frac{R}{p} \left[Z + \left(\frac{\partial Z}{\partial T} \right)_p T \right] \quad (30)$$

where,

$$C_3 = \sum_{n=13}^{58} (C_n^{*'} D_n^*), \quad (31)$$

$$D_n = (b_n - c_n k_n \rho_r^{k_n}) \rho_r^{b_n} e^{-c_n \rho_r^{k_n}}, \quad (32)$$

$$\left(\frac{\partial Z}{\partial T} \right)_p = \frac{R(TZ)^2 C_3 - pZ[TK^3 C_0 + C_4]}{R(TZ)^2 + pTC_4}, \quad (33)$$

$$C_4 = C_5 + \sum_{n=13}^{58} C_n^* D_{1n} \quad (34)$$

$$C_5 = B - K^3 \sum_{n=13}^{18} C_n^* \quad (35)$$

and

$$D_{1n} = K^3 [b_n^2 - c_n k_n (2b_n + k_n - c_n k_n \rho_r^{k_n}) \rho_r^{k_n}] \times \rho_r^{b_n - 1} e^{-c_n \rho_r^{k_n}}. \quad (36)$$

The isentropic exponent is defined by the following relation

$$\kappa = -\frac{c_{m,p}}{c_{m,v}} \left(\frac{\partial p}{\partial v_m} \right)_T \left(\frac{v_m}{p} \right) = -\frac{c_{m,p}}{c_{m,v} \rho_m p} \left(\frac{\partial p}{\partial v_m} \right)_T, \quad (37)$$

where

$$\begin{aligned} \left(\frac{\partial p}{\partial v_m} \right)_T &= \left(\frac{\partial p}{\partial \rho_m} \right)_T \left(\frac{\partial \rho_m}{\partial v_m} \right)_T \\ &= -RT \rho_m^2 (Z + \rho_m C_4). \end{aligned} \quad (38)$$

The Joule–Thomson coefficient is defined by the following equation [2]:

$$\mu_{JT} = \frac{RT^2}{p c_{m,p}} \left(\frac{\partial Z}{\partial T} \right)_p. \quad (39)$$

The derivation of the Eq. (39) is given in [6] and [7].

3. Implementation

The procedure for the calculation of the natural gas density, compression, molar heat capacity, isentropic exponent, and the Joule–Thomson coefficient is implemented in the OOP mode, which enables an easy integration into new software projects. The interface to the software object is shown in Fig. 2. The input/output parameters and functions are accessible, while the internal structure is hidden from the user. The function “Calculate” maps the input parameters (pressure, temperature, and the molar fractions of natural gas components) into the output parameters (density, compression, molar heat capacity, isentropic exponent, and Joule–Thomson coefficient). Table 3 depicts the calculation procedure. Prior to the calculation of the molar heat capacities, the isentropic exponent, and the Joule–Thomson coefficient, the density and the compression factor of a natural gas must be calculated. The false position method is combined with the successive bisection method to calculate the roots of the equation of state [4]. Using CORBA [8] or DCOM [9], the component can be accessed remotely.

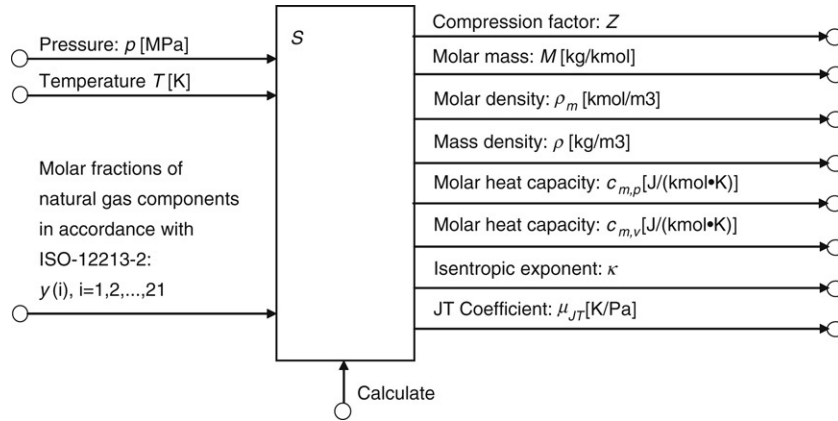


Fig. 2. Interface to the software object that implements the calculation of the natural gas properties.

Table 3

The input/output parameters and the procedure for the computation of the natural gas properties

Input parameters—constant:

- Molar gas constant ($R = 8314.51 \text{ J}/(\text{kmol K})$)
- Natural gas equation of state parameters ($a_n, b_n, c_n, k_n, u_n, g_n, q_n, f_n, s_n, w_n; n = 1, 2, \dots, 58$), characterization parameters ($M_i, E_i, K_i, G_i, Q_i, F_i, S_i, W_i; i = 1, \dots, 21$) and binary interaction parameters ($E_{i,j}^*, U_{i,j}, K_{i,j}, G_{i,j}^*$) (see ISO 12213-2)
- DIPPR/AIChE gas heat capacity constants ($a_j, b_j, c_j, d_j, e_j; j = 1, 2, \dots, N$)

Input parameters—time varying:

- Absolute pressure: p (MPa)
- Absolute temperature: T (K)
- Molar fractions of the natural gas mixture: $y_i; i = 1, 2, \dots, N$

Calculation procedure:

- 1 Mixture size parameter K (Eq. (13)), second virial coefficient B (Eq. (14)) and temperature dependent coefficients C_n^* (Eq. (18))
- 2 Compression factor Z (Eq. (8)) (see ISO-12213-2 for details of calculation)
- 3 Molar density $\rho_m = p/RTZ$, reduced density $\rho_r = K^3 \rho_m$ and molar volume $v_m = 1/\rho_m$.
- 4 Coefficients D_n and D_{1n} (Eqs. (32) and (36))
- 5 1st and 2nd derivative of the second virial coefficient $B: B'$ (Eq. (23)) and B'' (Eq. (24))
- 6 1st and 2nd derivative of the coefficient $C_n^* : C_n^{*'} (Eq. (25))$ and $C_n^{*''} (Eq. (26))$
- 7 1st derivative of the compression factor $Z : (\partial Z/\partial T)_p$ (Eq. (33))
- 8 Partial derivatives of pressure: $(\partial p/\partial T)_{v_m}$ (Eq. (29)) and $(\partial p/\partial v_m)_T$ (Eq. (38))
- 9 Ideal molar heat capacity of a gas mixture at constant pressure: $c_{m,pI}$ (Eq. (27))
- 10 Molar heat capacity of a gas mixture at constant volume: $c_{m,v}$ (Eq. (9))
- 11 Molar heat capacity of a gas mixture at constant pressure: $c_{m,p}$ (Eq. (4))
- 12 Isentropic exponent κ (Eq. (37))
- 13 Joule–Thomson coefficient μ_{JT} (Eq. (39))

4. Application

We investigated the combined effect of the Joule–Thomson coefficient and the isentropic exponent of a natural gas on the accuracy of flow-rate measurements based on differential devices. The measurement of a natural gas [4] flowing in a pipeline through an orifice plate with corner taps (Fig. 1) is assumed to be completely in accordance with the international standard ISO-5167-2 [10]. The detailed description of the flow-rate equation with the corresponding iterative computation

scheme is given in [2] and [10]. The flow-rate through the orifice is proportional to the expansibility factor, which is related to the isentropic exponent. According to [10], the expansibility factor ε for the orifice plate with corner taps is defined by:

$$\varepsilon = 1 - (0.351 + 0.256\beta^4 + 0.93\beta^8)[1 - (p_2/p_1)^{1/\kappa}] \quad (40)$$

where β denotes the ratio of the diameter of the orifice to the internal diameter of the pipe, while p_1 and p_2 are the absolute pressures upstream and downstream of the orifice plate, respectively. The corresponding temperature change ΔT of the gas for the orifice plate with corner taps is defined by

$$\Delta T = T_1 - T_2 \approx \mu_{JT}(p_1, T_2)\Delta\omega \quad (41)$$

where T_1 and T_2 indicate the corresponding temperatures upstream and downstream of the orifice plate, $\mu_{JT}(p_1, T_2)$ is the Joule–Thomson coefficient at upstream pressure p_1 and downstream temperature T_2 , and $\Delta\omega$ is the pressure loss across the orifice plate [11], defined by

$$\Delta\omega = \frac{\sqrt{1 - \beta^4(1 - C^2)} - C\beta^2}{\sqrt{1 - \beta^4(1 - C^2)} + C\beta^2} \Delta p \quad (42)$$

where C denotes the coefficient of discharge for the orifice plate with corner taps [10], and ΔP is the pressure drop across the orifice plate. According to [2], the temperature of the fluid shall preferably be measured downstream of the primary device, but upstream temperature shall be used for the calculation of the flow-rate. Within the limits of the application of ISO-5167 [2], it is generally assumed that the temperature drop across the differential device can be neglected, but it is also suggested that it be taken into account if higher accuracies are required. It is also assumed that the isentropic exponent can be approximated by the ratio of the specific heat capacity at constant pressure to the specific heat capacity at constant volume of the ideal gas. The above approximations may produce a measurement error. The relative flow measurement error E_r is estimated by comparing the approximate (q_{m2}) and the corrected (q_{m1}) mass flow-rate i.e.

$$E_r = (q_{m2} - q_{m1})/q_{m1}. \quad (43)$$

Table 4

The procedure for the correction of the mass flow-rate due to adiabatic expansion effects

| Step | Description |
|------|--|
| 1 | Calculation of Joule–Thomson coefficient $\mu_{JT}(p_1, T_2)$ by using the procedure outlined in Table 3 with upstream pressure p_1 and downstream temperature T_2 |
| 2 | Estimation of upstream temperature T_1 using the Eq. (41) |
| 3 | Calculation of density $\rho = M\rho_m$ and isentropic exponent κ using the procedure outlined in Table 3 with upstream pressure p_1 and estimated upstream temperature T_1 |
| 4 | Calculation of viscosity (residual viscosity function) [12] |
| 5 | Calculation of mass flow-rate in accordance with [10] |

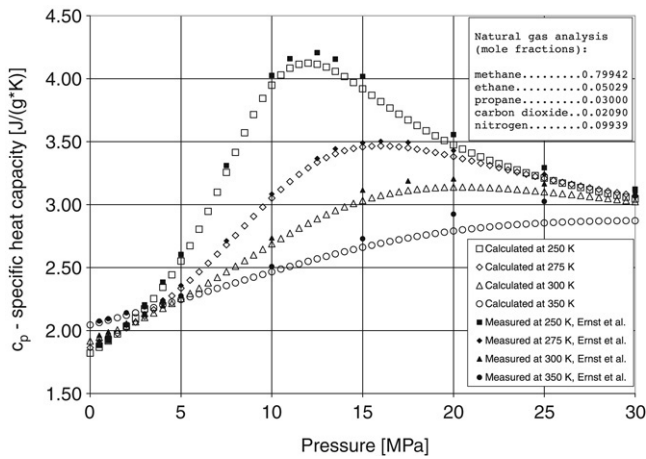


Fig. 3. Calculated and measured molar heat capacities at constant pressure of the natural gas mixture.

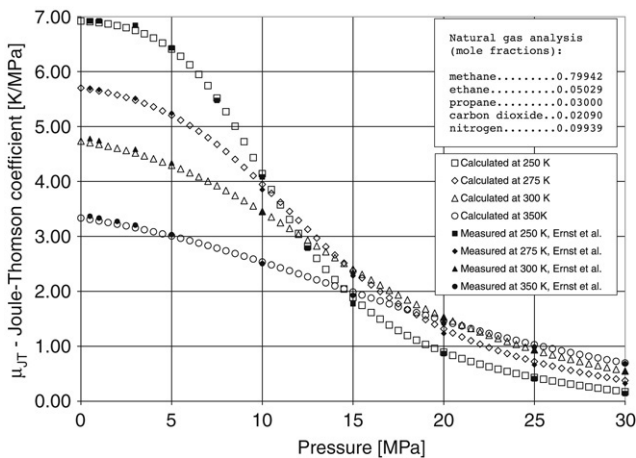


Fig. 4. Calculated and measured Joule–Thomson coefficients of the natural gas mixture.

The individual and the combined relative errors due to the approximations of the temperature drop and the isentropic exponent are calculated. The procedure for the correction of the mass flow-rate due to the adiabatic expansion effects is shown in Table 4. The calculation procedures are implemented in the OOP mode. The results are presented in the following section.

Table 5

Difference between the calculated and measured specific heat capacity at constant pressure of a natural gas

| P (MPa): T (K) | 250 | 275 | 300 | 350 |
|--------------------|---|--------|--------|--------|
| | $(c_p \text{ calculated} - c_p \text{ measured})$ (J/(g * K)) | | | |
| 0.5 | -0.015 | -0.018 | -0.018 | -0.012 |
| 1.0 | -0.002 | -0.014 | -0.016 | -0.011 |
| 2.0 | -0.012 | -0.019 | -0.022 | -0.020 |
| 3.0 | -0.032 | -0.020 | -0.023 | -0.026 |
| 4.0 | -0.041 | -0.023 | -0.021 | -0.027 |
| 5.0 | -0.051 | -0.022 | -0.025 | -0.029 |
| 7.5 | -0.055 | -0.032 | - | - |
| 10.0 | -0.077 | -0.033 | -0.048 | -0.042 |
| 11.0 | -0.075 | - | - | - |
| 12.5 | -0.092 | -0.030 | - | - |
| 13.5 | -0.097 | -0.039 | - | - |
| 15.0 | -0.098 | -0.033 | -0.082 | -0.069 |
| 16.0 | - | -0.036 | - | - |
| 17.5 | - | -0.043 | -0.075 | - |
| 20.0 | -0.081 | -0.048 | -0.066 | -0.134 |
| 25.0 | -0.082 | -0.033 | -0.064 | -0.171 |
| 30.0 | -0.077 | -0.025 | -0.070 | -0.194 |

Table 6

Difference between the calculated and measured Joule–Thomson coefficient of a natural gas

| P (MPa): T (K) | 250 | 275 | 300 | 350 |
|--------------------|---|--------|--------|--------|
| | $(\mu_{JT} \text{ calculated} - \mu_{JT} \text{ measured})$ (K/MPa) | | | |
| 0.5 | -0.014 | -0.023 | -0.075 | -0.059 |
| 1.0 | -0.032 | -0.024 | -0.068 | -0.053 |
| 2.0 | - | - | - | -0.051 |
| 3.0 | -0.092 | -0.032 | -0.069 | -0.049 |
| 5.0 | -0.022 | -0.036 | -0.044 | -0.026 |
| 7.5 | 0.043 | - | - | - |
| 10.0 | 0.060 | 0.096 | 0.019 | 0.030 |
| 12.5 | 0.034 | - | - | - |
| 15.0 | 0.113 | 0.093 | 0.050 | 0.061 |
| 20.0 | 0.029 | 0.084 | 0.009 | 0.047 |
| 25.0 | 0.025 | 0.059 | 0.002 | 0.043 |
| 30.0 | 0.031 | 0.052 | 0.005 | 0.012 |

5. Measurement results

In order to compare the measurement results, for the specific heat capacity c_p and the Joule–Thomson coefficient μ_{JT} , with the corresponding high accuracy measurement data [13] (Ernst et al.), we assume identical artificial natural gas mixtures with the following mole fractions: $x_{CH_4} = 0.79942$, $x_{C_2H_6} = 0.05029$, $x_{C_3H_8} = 0.03000$, $x_{CO_2} = 0.02090$, and $x_{N_2} = 0.09939$. The results of the measurements [13] and the results of the calculation of the specific heat capacities c_p and the Joule–Thomson coefficients μ_{JT} of the natural gas mixtures, for absolute pressures ranging from 0 to 30 MPa in 0.5 MPa steps and for four upstream temperatures (250, 275, 300, and 350 K), are shown in Fig. 3 and Fig. 4, respectively. The differences between the calculated values and the corresponding measurement results [13], for c_p and μ_{JT} , are shown in Table 5 and Table 6, respectively. From Table 5, it can be seen that the calculated values of c_p are within ± 0.08 J/(g * K) of the measurement results for pressures up

to 12 MPa. At higher pressures, up to 30 MPa, the difference increases, but never exceeds $\pm 0.2 \text{ J}/(\text{g} \cdot \text{K})$. For pressures up to 12 MPa, the relative difference between the calculated and experimentally obtained c_p never exceeds $\pm 2.00\%$. From Table 6, it can be seen that the calculated values of μ_{JT} are within $\pm 0.113 \text{ K}/\text{MPa}$, with the experimental results for the pressures up to 30 MPa. The relative difference increases with the increase in pressure, but never exceeds $\pm 2.5\%$ for pressures up to 12 MPa. At higher pressures, when the values of μ_{JT} are close to zero, the relative difference may increase significantly. The results of the calculations obtained for pure methane and methane–ethane mixtures are in considerably better agreement with the corresponding experimental data [13] than those for the natural gas mixture shown above. We estimate that the relative uncertainties of the calculated c_p and μ_{JT} of the AGA-8 natural gas mixtures in common industrial operating conditions (pressure range 0–12 MPa and temperature range 250–350 K) are unlikely to exceed $\pm 3.00\%$ and $\pm 4.00\%$, respectively. Fig. 5 shows the results of the calculation of the isentropic exponent. Since the isentropic exponent is a theoretical parameter, there exist no experimental data for its verification.

In order to simulate a flow-rate measurement error caused by an inappropriate compensation for the adiabatic expansion, a natural gas mixture (Gas 3) from Annex C of [4] is assumed to flow through the orifice plate with corner taps [9] shown in Fig. 1. Following the recommendations [2], the absolute pressure is assumed to be measured upstream (p_1), and the temperature downstream (T_2), of the primary device. A natural gas analysis in mole fractions is the following: methane 0.859, ethane 0.085, propane 0.023, carbon dioxide 0.015, nitrogen 0.010, i-butane 0.0035, n-butane 0.0035, i-pentane 0.0005, and n-pentane 0.0005. Fig. 6 illustrates the temperature drop due to the Joule–Thomson effect calculated in accordance with Eq. (41). The results calculated are given for two discrete differential pressures, Δp (20 and 100 kPa), for absolute pressures p_1 ranging from 1 to 60 MPa in 1 MPa steps, and for six equidistant upstream temperatures T_1 in the range from 245 to 345 K. From Fig. 6 it can be seen that for each temperature there exists the corresponding pressure where the Joule–Thomson coefficient changes its sign, and consequently alters the sign of the temperature change. A relative error in the flow-rate measurements (Fig. 1) due to the Joule–Thomson effect is shown in Fig. 7. The error is calculated in accordance with Eq. (43) by comparing the approximate mass flow-rate (q_{m2}) with the corrected mass flow-rate (q_{m1}). The procedure for the precise correction of the mass flow-rate is shown in Table 4. The approximate flow-rate and the corresponding natural gas properties (density, viscosity, and isentropic exponent) are calculated at upstream pressure p_1 , downstream temperature T_2 , and differential pressure Δp , by neglecting the temperature drop due to the Joule–Thomson effect ($T_2 = T_1$). The results are shown for two discrete differential pressures Δp (20 and 100 kPa), for absolute upstream pressures p_1 ranging from 1 to 60 MPa in 1 MPa steps, and for four equidistant downstream temperatures T_2 in the range from 245 to 305 K.

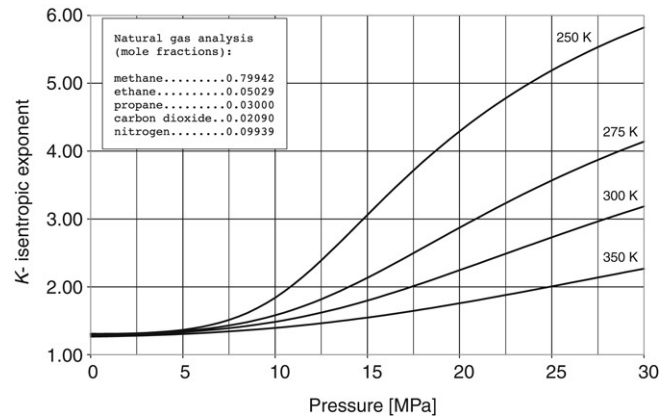


Fig. 5. Calculated isentropic exponent of the natural gas mixture.

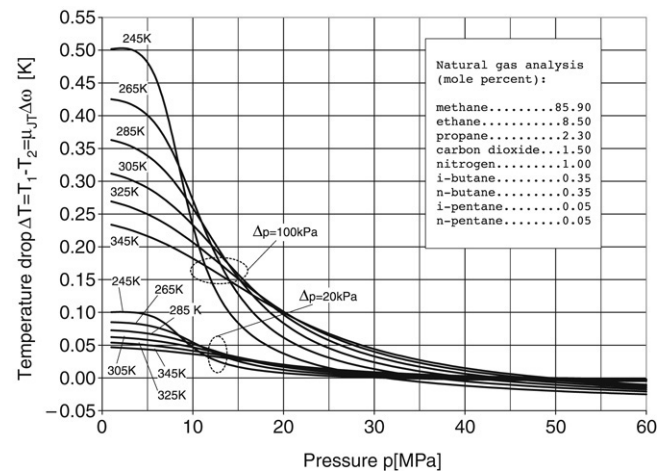


Fig. 6. Temperature drop due to the Joule–Thomson effect $\Delta T = \mu_{JT}\Delta p$ when measuring flow-rate of the natural gas mixture through the orifice plate with corner taps (ISO-5167-2). The upstream pressure varies from 1 to 60 MPa in 1 MPa steps and upstream temperature from 245 to 305 K in 20 K steps for each of two differential pressures Δp (20 and 100 kPa). The internal diameters of the orifice and pipe are: $d = 120 \text{ mm}$ and $D = 200 \text{ mm}$.

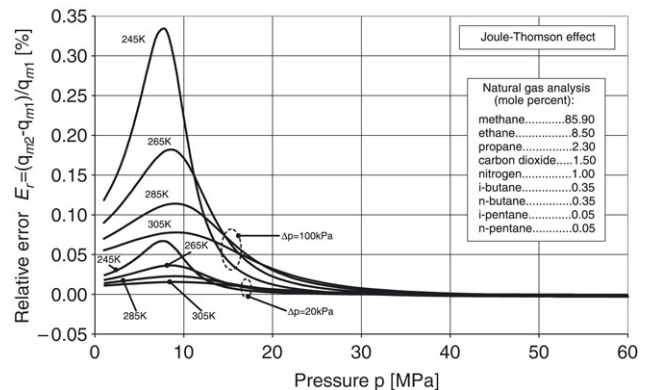


Fig. 7. Relative error $E_r = (q_{m2} - q_{m1})/q_{m1}$ in the flow-rate of the natural gas mixture measured by the orifice plate with corner taps (ISO-5167-2) when using downstream temperature with no compensation for the Joule–Thomson effect (q_{m2}) instead of upstream temperature (q_{m1}). The upstream pressure varies from 1 to 60 MPa in 1 MPa steps, and downstream temperature from 245 to 305 K in 20 K steps for each of two differential pressures Δp (20 and 100 kPa). The internal diameters of the orifice and pipe are: $d = 120 \text{ mm}$ and $D = 200 \text{ mm}$.

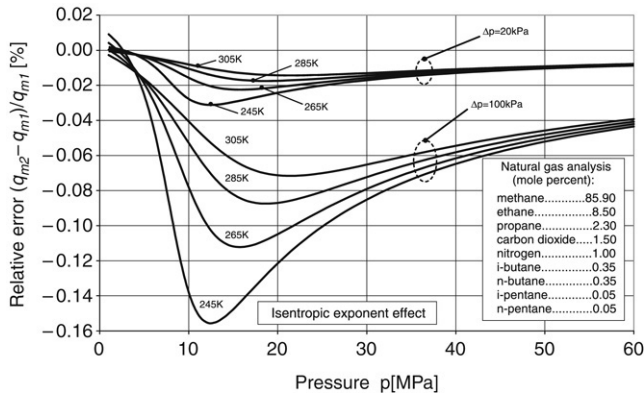


Fig. 8. Relative error $E_r = (q_{m2} - q_{m1})/q_{m1}$ in the flow-rate of the natural gas mixture measured by the orifice plate with corner taps (ISO-5167-2) when using the isentropic exponent of the ideal gas (q_{m2}) instead of the real gas (q_{m1}). The upstream pressure varies from 1 to 60 MPa in 1 MPa steps, and downstream temperature from 245 to 305 K in 20 K steps, for each of two differential pressures Δp (20 and 100 kPa). The internal diameters of the orifice and pipe are: $d = 120$ mm and $D = 200$ mm.

Fig. 8 illustrates the relative error in the flow-rate measurements due to the approximation of the isentropic exponent by the ratio of the ideal molar heat capacities. The error is calculated by comparing the approximate mass flow-rate (q_{m2}) with the corrected mass flow-rate (q_{m1}) in accordance with Eq. (43). The procedure for the precise correction of the mass flow-rate is shown in Table 4. The approximate flow-rate calculation is carried out in the same way, with the exception of the isentropic exponent, which equals the ratio of the ideal molar heat capacities ($\kappa = c_{m,p1}/(c_{m,p1} - R)$). The results are shown for two discrete differential pressures Δp (20 and 100 kPa), for absolute upstream pressures p_1 ranging from 1 to 60 MPa in 1 MPa steps, and for four equidistant downstream temperatures T_2 in the range from 245 to 305 K.

Fig. 9 shows the flow-rate measurement error produced by the combined effect of the Joule–Thomson and the isentropic expansions. The error is calculated by comparing the approximate mass flow-rate (q_{m2}) with the corrected mass flow-rate (q_{m1}) in accordance with Eq. (43). The procedure for the precise correction of the mass flow-rate is shown in Table 4. The approximate flow-rate and the corresponding natural gas properties are calculated at upstream pressure p_1 , downstream temperature T_2 , and differential pressure Δp , by neglecting the temperature drop due to the Joule–Thomson effect ($T_2 = T_1$) and by substituting the isentropic exponent with the ratio of the ideal molar heat capacities, $\kappa = c_{m,p1}/(c_{m,p1} - R)$. The results are shown for two discrete differential pressures Δp (20 and 100 kPa), for absolute upstream pressures p_1 ranging from 1 to 60 MPa in 1 MPa steps, and for four equidistant downstream temperatures T_2 in the range from 245 to 305 K.

The results obtained for the Joule–Thomson coefficient and isentropic exponent are in complete agreement with the results obtained when using the procedures described in [7] and [14], which use natural gas fugacities to derive the molar heat capacities and are, therefore, considerably more computationally intensive and time consuming. The

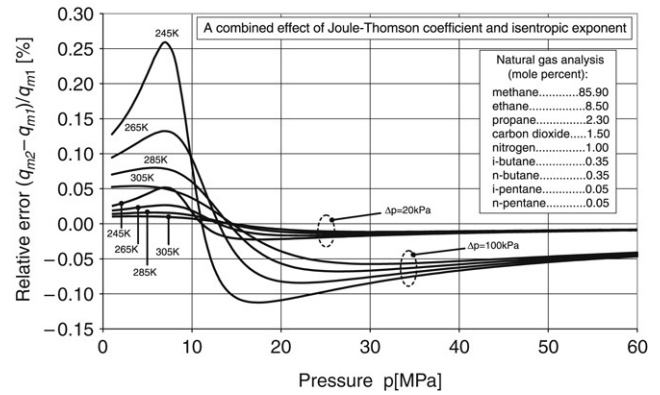


Fig. 9. Relative error $E_r = (q_{m2} - q_{m1})/q_{m1}$ in the flow-rate of the natural gas mixture measured by an orifice plate with corner taps (ISO-5167-2) when using downstream temperature, with no compensation for the Joule–Thomson effect and the isentropic exponent of the ideal gas at downstream temperature (q_{m2}) instead of upstream temperature, and the corresponding real gas isentropic exponent (q_{m1}). The upstream pressure varies from 1 to 60 MPa in 1 MPa steps and downstream temperature from 245 to 305 K in 20 K steps for each of two differential pressures Δp (20 and 100 kPa). The internal diameters of the orifice and pipe are: $d = 120$ mm and $D = 200$ mm.

calculation results are shown up to a pressure of 60 MPa, which lies within the wider ranges of application given in [4], of 0–65 MPa. However, the lowest uncertainty for compressibility is for pressures up to 12 MPa, and no uncertainty is quoted in Reference [4] for pressures above 30 MPa. It would therefore seem sensible for the results of the Joule–Thomson and the isentropic exponent calculations to be used with caution above this pressure. From Fig. 9 it can be seen that the maximum combined error is lower than the maximum individual errors, because the Joule–Thomson coefficient (Fig. 7) and the isentropic exponent (Fig. 8) show the countereffects on the flow-rate error. The error always increases by decreasing the operating temperature. The total measurement error is still considerable, especially at lower temperatures and higher differential pressures, and cannot be overlooked. The measurement error is also dependent on the natural gas mixture. For certain mixtures, like natural gases with a high carbon dioxide content, the relative error in the flow-rate may increase up to 0.5% at lower operating temperatures (245 K), and up to 1.0% at very low operating temperatures (225 K). Whilst modern flow computers have a provision for applying a Joule–Thomson coefficient and an isentropic exponent correction to measured temperatures, this usually takes the form of a fixed value supplied by the user. The calculations in this paper show that any initial error in choosing this value, or subsequent operational changes in temperature, pressure or gas composition, could lead to significant systematic metering errors. Our further work will be directed towards the improvement of the model, with the aim of simplifying the calculation procedure and further decreasing the uncertainty of the calculation results.

6. Conclusion

This paper describes the numerical procedure for the calculation of the natural gas molar heat capacity, the

Joule–Thomson coefficient and the isentropic exponent. The corresponding equations have been derived by applying the fundamental thermodynamic relations to AGA-8 extended virial-type equations of state. The DIPPR AIChE generic ideal heat capacity equations have been used to calculate the ideal molar heat capacities of a natural gas mixture. The implementation of the procedure in an OOP mode enables its easy integration into new software developments. An example of a possible application of the procedure in the flow-rate measurements has been given. The procedure can be efficiently applied in both off-line calculations and real time measurements.

Acknowledgements

This work has been supported by the Croatian Ministry of Science, Education, and Sport with the projects “Computational Intelligence Methods in Measurement Systems” and “Real-Life Data Measurement and Characterization”. The author would like to express his thanks to Professor Donald R. Olander, University of California, Berkeley, USA, for his valuable suggestions, and to Dr. Eric W. Lemmon, NIST, USA, for his help in obtaining the relevant measurement data.

References

- [1] Shoemaker DP, Garland CW, Nibler JW. Experiments in physical chemistry. 6th ed. New York: McGraw-Hill; 1996.
- [2] ISO-51671-1. Measurement of fluid flow by means of pressure differential devices inserted in circular-cross section conduits running full — Part 2: General principles and requirements. Ref. No. ISO-51671-1:2003(E). ISO; 2003.
- [3] AGA 8. Compressibility and supercompressibility for natural gas and other hydrocarbon gases. Transmission measurement committee report no. 8, AGA catalog no. XQ 1285. Arlington (Va.); 1992.
- [4] ISO-12213-2. Natural gas – calculation of compression factor – Part 2: Calculation using molar-composition analysis. Ref. No. ISO-12213-2:1997(E). ISO; 1997.
- [5] DIPPR[®] 801. Evaluated standard thermophysical property values, Design Institute for Physical Properties. Sponsored by AIChE. 2004.
- [6] Olander DR. Thermodynamic relations. In: Engineering thermodynamics, Retrieved September 21, 2005, from Department of Nuclear Engineering, University of California: Berkeley [Chapter 7]. WEB site: <http://www.nuc.berkeley.edu/courses/classes/E-115/Reader/index.htm>.
- [7] Marić I. The Joule–Thomson effect in natural gas flow-rate measurements. Flow Measurement and Instrumentation 2005;16:387–95.
- [8] Vinoski S. CORBA: Integrating diverse applications within distributed heterogeneous environments. IEEE Communications Magazine 1997; 35(2):46–55.
- [9] Microsoft: DCOM Architecture. White Paper. Microsoft Corporation. 1998.
- [10] ISO-51671-2. Measurement of fluid flow by means of pressure differential devices inserted in circular-cross section conduits running full — Part 2: Orifice plates. Ref. No. ISO-51671-2:2003(E). ISO; 2003.
- [11] Urner G. Pressure loss of orifice plates according to ISO-5167. Flow Measurement and Instrumentation 1997;8:39–41.
- [12] Miller RW. The flow measurement engineering book. 3rd ed. New York: McGraw-Hill; 1996.
- [13] Ernst G, Keil B, Wirbser H, Jaeschke M. Flow calorimetric results for the massic heat capacity c_p and Joule–Thomson coefficient of CH_4 , of $(0.85\text{CH}_4 + 0.16\text{C}_2\text{H}_6)$, and of a mixture similar to natural gas. Journal of Chemical Thermodynamics 2001;33:601–13.
- [14] Marić I, Galović A, Šmuc T. Calculation of natural gas isentropic exponent. Flow Measurement and Instrumentation 2005;16(1):13–20.